

This paper was presented at the 10th International Conference on Cold Fusion. It may be different from the version published by World Scientific, Inc (2003) in the official Proceedings of the conference.

Development of Compact Nuclear Fusion Reactor Using Solid Pycnodeuterium as Nuclear Fuel

Yoshiaki Arata and Yue Chang Zhang
Cooperation Research Center for Science and Technology, Osaka University
2-1, Yamadaoka, Suita, Osaka, 565-0871, Japan

Abstract

Based on the functioning of Pd black inside a DS-Cathode, which has produced irrefutable evidence for the existence of solid nuclear fusion, new materials were developed to absorb abundant D/H atoms, up to levels as high as 300% of Pd number. These absorbed atoms were solidified densely inside each unit cell of the host lattice as solid-state “Pycnodeuterium” or “Pycnohydrogen.” Stimulation energy with Pycnodeuterium easily caused intense solid-state nuclear fusion, whereas with Pycnohydrogen no reaction occurred. As the result, it was clarified that Pycnodeuterium is by far the best nuclear fuel compared to all other nuclear fuels.

Introduction

We thoroughly studied this phenomenon over more than ten years (1990 - 2002) to make clear in detail characteristics of Pd black inside a DS-cathode (Double Structure Cathode) compared against bulk Pd¹⁾. As a result, the essential conditions necessary to induce nuclear fusion by Pycnodeuterium formed within surface zone of Pd black were obtained based on the experiments described below.

1) Amount of D/H atoms absorbed into Pd black.

It is well known that the amount of D/H-atoms absorbed into a metal absorbent can be obtained using Sieverts' law. We studied in detail some characteristics of absorption of D/H-atoms into Pd black¹⁾. The most important steps in the experimental method used were: first, keep Pd black inside a fixed vacuum vessel ($\sim 10^{-7}$ Torr) at constant temperature for 2~3 days, and second, inject D₂/H₂ gas into the vacuum vessel at a constant low flow rate like 20 cc/min.

a) Existence of “incubation period”

In elucidating the D₂/H₂ absorption characteristics, two important kinds of behavior regarding Pd black were identified. As demonstrated in Fig 1 (next section), two kinds of materials were recognized: (A-material: no absorption of D₂/H₂, and B-material: abundantly absorbs D₂/H₂). With A-material, the inner pressure P_{in} (pressure inside the vacuum vessel) increases proportionally with increasing elapsed time τ during an “increasing period.” But with the B-material there is initially no increase in observed pressure with elapsed time. P_{in} shows no observed change during a “constant

period,” ending at point B_0 on the horizontal axis. At the end of time period B_0 a saturated-state of D/H atoms in the nano-metal is reached, corresponding to elapsed time $\tau = \tau_0$. Then P_{in} suddenly starts to increase, and continues to increase throughout time period B_1 , which begins at $\tau = \tau_0$. In other words, in B-material, two kinds of time periods in measured pressure P_{in} were observed (“constant period” B_0 and “increasing period” B_1). We use the name “incubation period” for the “constant period” with no increase in observed P_{in} above the zero reading. The incubation period extends from $\tau = \tau_0$ (starting point) to $\tau = \sim \tau_0$. The observations showed that Pd black corresponds to B-material, whereas the bulk state of all metals corresponds to A-material.

b) Importance of Particle size

We clarified the relations between the incubation period measured by τ_0 , the amount of D_2/H_2 -absorbed at low pressure, and the Pd particle size, as shown in Fig. A, taken from Fig. 2A in *Proc. Japan Acad.* **71B** (1995)²⁾. It was concluded that both the volume of the surface zone of Pd black and the amount of D/H atoms which are easily absorbed inside the Pd black increase greatly with decreasing grain size in the Pd black. In other words, it is best to have as small a particle size as possible. This means that the surface zone of Pd black plays the essential role in causing solid nuclear fusion. These results led us to develop new materials which form abundant “Pycnodeuterium,” so as to cause solid nuclear fusion³⁾. Using Pd black with extremely small particle size (150 ~ 400Å in size) inside DS-cathode, it was observed that Pycnodeuterium caused intense solid nuclear fusion ($>10^{15}$ 4He atoms generated in closed inner space of DS-cathode). In contrast, neither Pycnohydrogen and nor bulk Pd ever caused any solid nuclear fusion, as shown in Fig. B¹⁾. We have performed a new project which has added to these experimental facts.

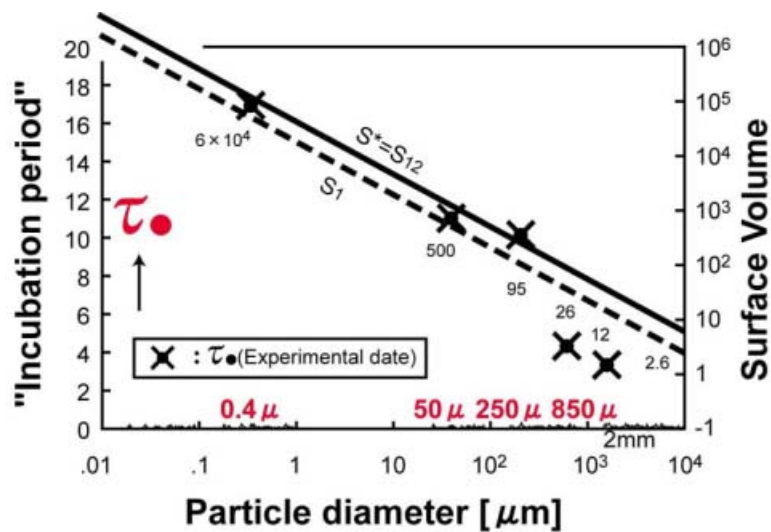


Fig. A. Importance of Pd particle size

Conclusion

Nuclear Fusion Resulted from DS-Cathode

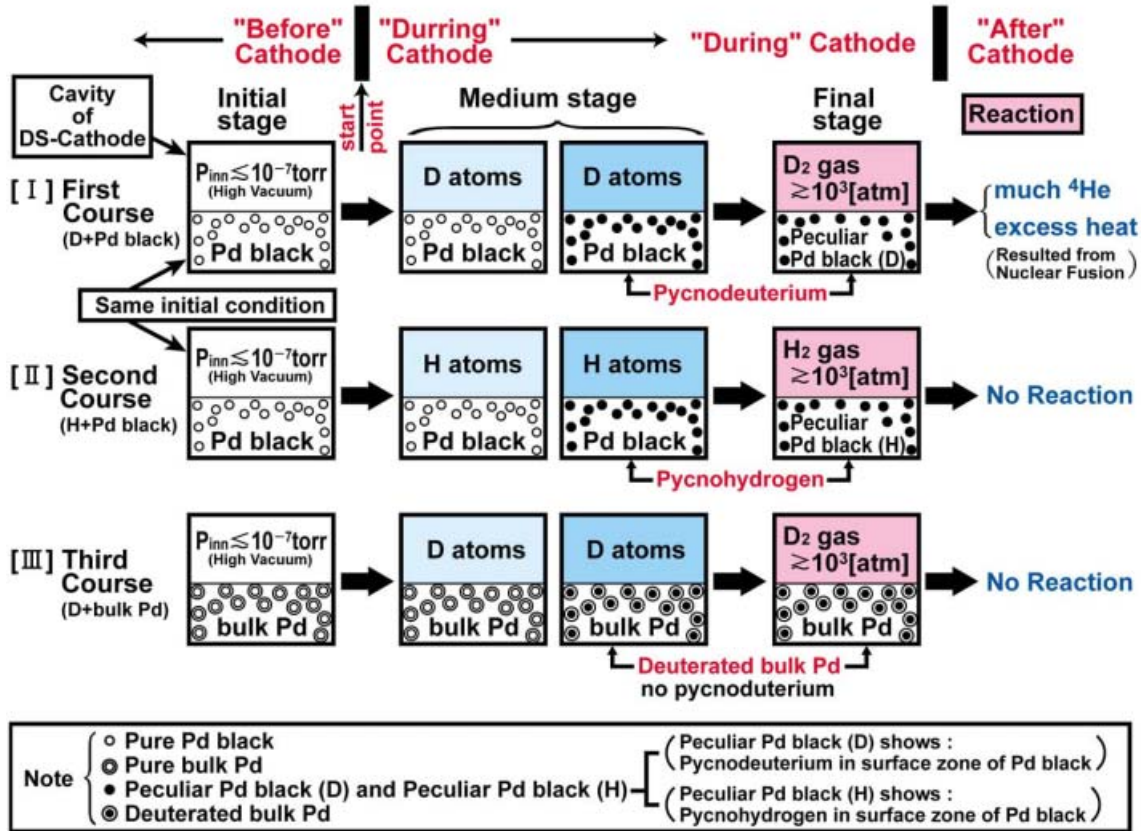


Fig. B. Comparison of Pycnodeuterium and Pycnohydrogen, also between Pd black and bulk Pd. In only [I] (First Course); that is, Pycnodeuterium generated in surface zone of Pd black absorbed D-atoms caused intense solid nuclear fusion, but in other [II] and [III] course, made no events.

Absorption Experiment

The most important information gained from the absorption experiments using Pd black inside DS-cathodes was the existence of an incubation period, as described in detail in the introduction. We have developed new materials with long incubation periods (as long as possible).

Fig. 1 shows a typical example of the relation between the characteristics of materials and their incubation periods. The new experiments were designed to produce the next important experimental result (Fig. 4). In these studies D₂ gas was injected at a constant rate, such as 20 cc/min, until P_{in} built up to 10 atm within the closed vacuum vessel. Two kinds of materials illustrate extreme behaviors. In A–material there is no noticeable initial gas absorption in the metal, as shown by the immediate onset of pressure rise and by the lack of chemical reaction heat. In contrast, B–material strongly absorbs gas even under partial vacuum conditions. The pressure rise curve for B–material shows two behavior periods. The first period records no rise in P_{in} with elapsed time. P_{in} follows along the horizontal axis until it reaches point b₀, which marks the end of the incubation period. The second period begins with point b₀, which initiates an interval of rising P_{in}. The onset of rising pressure means that the D-atom concentration reached saturation inside the material at point b₀. B–material is also characterized by a large release of chemical energy during the first period, as shown in curve C. The heat release results from the exothermic absorption of D-atoms. The heat release corresponds to ~10 kcal/mol throughout the incubation period. As a result, the exact amount of absorbed D-atoms is easily calculated based on incubation period observation.

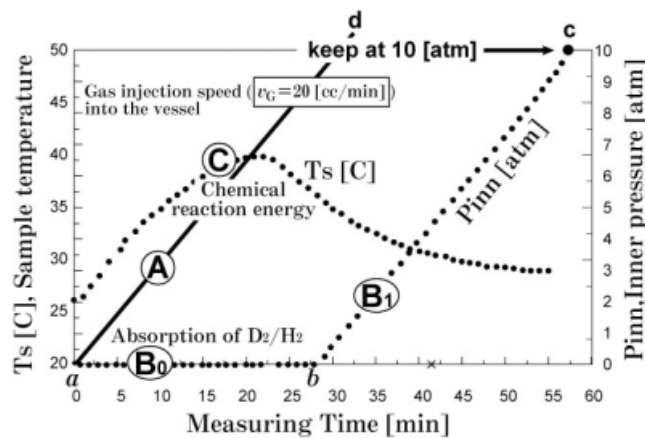


Fig.1 Typical Characteristics of D₂/H₂ Absorption into Sample powder kept inside evacuated Vessel

Note; [Material (A): no absorption of D₂/H₂
 [Material (B) (B₀, B₁): intense absorption of D₂/H₂

In one of the experiments, nano-Pd particles of 50Å size are embedded inside a matrix of ZrO₂. In Figs. 3 and 4, the sample powder is designated ZrO₂•Pd[®]. It is derived from an oxidized amorphous alloy of Zr₆₅Pd₃₅. ZrO₂ by itself behaves as A–material, while nano-Pd particles Pd[®] correspond to B–material. The nano-Pd easily absorbs about 3 D-atoms per host Pd[®] atom. These D-atoms are solidified as an ultrahigh density deuterium-lump (“Pycnodeuterium”) inside each octahedral space within unit cell of the Pd[®] host lattice. These “Pycnodeuterium” are dispersed so as to form a

“metallic deuterium lattice,” with body-centered cuboctahedron structure as shown in Fig. 2³⁾.

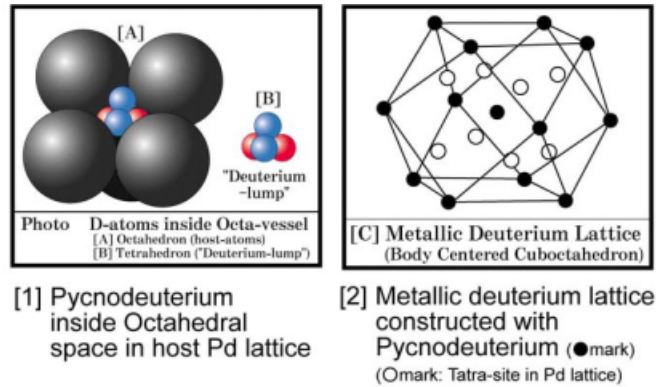


Fig. 2 Important Properties of "Pycnodeuterium"

Note; "Pycnodeuterium" is formed inside "nano-Pd" particles, peculiar oxidized and surface zone of "Pd black", but "bulk Pd" nothing one to form

$ZrO_2 \cdot Pd^\circ$ is one of the new materials, and moreover we developed bulk-state new material with the goal of achieving long incubation periods. For instance; new peculiar oxidized bulk composite such as a Zr-Ni-O system designated $Zr_3NiO \cdot NiO$ (shortly, $Zr^* \cdot NiO$ or Zr^* ; because $Zr^* \gg NiO$ in weight, then $Zr^* \equiv Zr_3NiO$) as shown in Fig 3 was developed. In this case, in order to realize a long incubation periods, we had to create bulk composite material Zr^* . Bulk-state metals never achieve long incubation periods, but bulk oxidized composite can absorb abundant D/H atoms. This composite is no metal and the whole of Zr^* is one crystal lattice of oxidized compound as “bulk-state”, on the contrary nano-metal Pd° is only a part of the sample. This is the biggest difference between nano Pd° and bulk Zr^* , but when the both samples absorb D/H atoms into their lattice, their constitutional host atoms work with similar mechanism as follows; each individual host atom of the nano-metal Pd° and each sub-unit of the bulk oxidized lattice of Zr^* releases strain energy stored within the atomic structure.

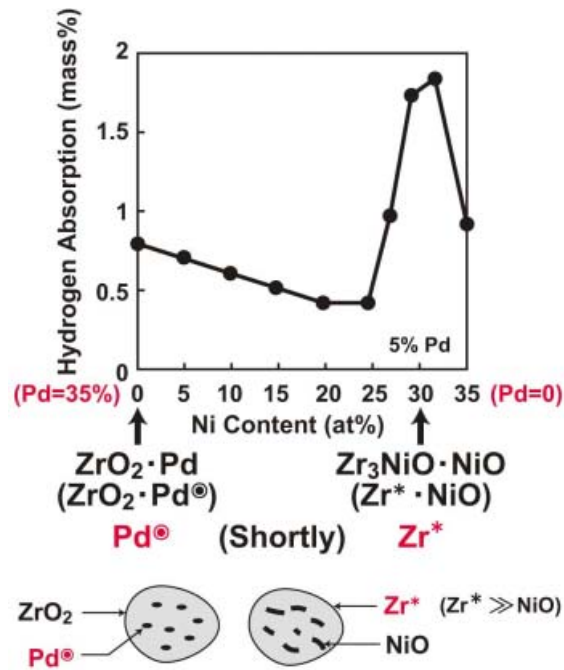


Fig. 3 Relation between sample powders of ZrO₂·Pd[⊙] and Zr*·NiO

Note: These sample are Oxidized powders of amorphous Zr₆₅Pd₃₅ and Zr₆₅Pd₅Ni₃₀, respectively.

Deuterium atoms are absorbed into only Pd[⊙]/Zr* (Pd[⊙]: nano-Pd, Zr*: bulk-Zr₃NiO)

In the same way as illustrated in Fig 1, we investigated the characteristics of the following sample powders, designated in Fig. 4 by their 4 kinds of materials: Zr*, Pd[⊙], Pd black (Pd[•]) and bulk metal Pd wire, designated Pd⁰. The wire was cut into pieces 0.2 mm in diameter and 2 mm in length. Each sample had a 3-gram weight. Results are shown in Fig. 4.

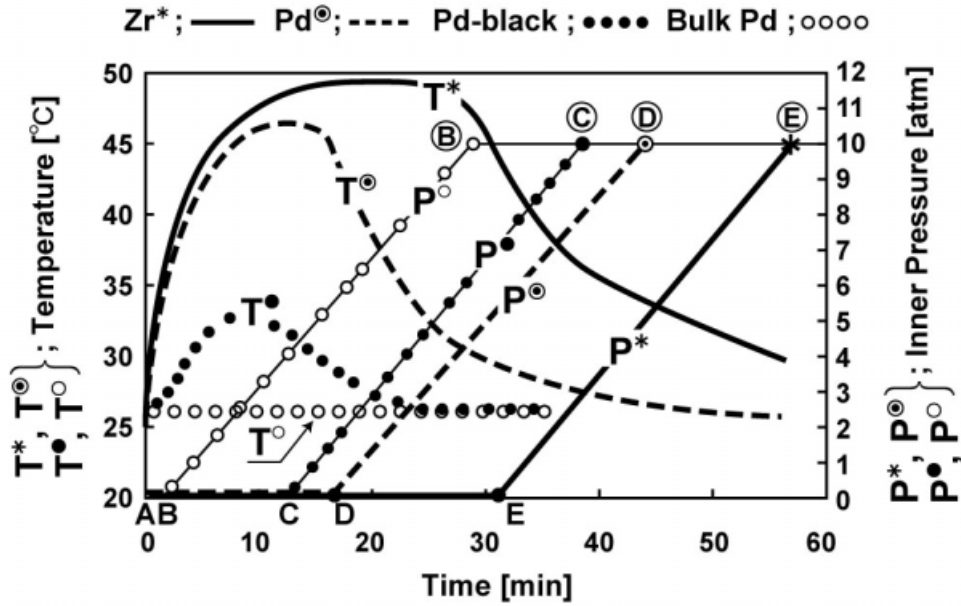


Fig. 4 Deuterium absorption characteristics of sample powders ; $Zr_3NiO \cdot NiO$ ($Zr^* \cdot NiO$), $ZrO_2 \cdot Pd(ZrO_2 \cdot Pd^\circ)$, Pd black and bulk Pd.

$Zr^* \cdot NiO > ZrO_2 \cdot Pd^\circ > Pd\text{-black} > Bulk Pd$
and $Zr^* \gg NiO$, $ZrO_2 = 0$, in D-absorption

$\therefore Zr^* > Pd^\circ > Pd\text{-black} > Bulk Pd$

$Zr^* (P^*, T^*) ; Pd^\circ (P^\circ, T^\circ) ; Pd\text{-black} (P^*, T^*) ; Bulk Pd (P^\circ, T^\circ)$

This diagram is one of the most important results in our chain of experiments. When the materials were used with the same total weight, bulk oxidized composite Zr^* absorbed the highest quantity of D-atoms, as indicated by the longest incubation period. It also generated the largest chemical reaction energy. In contrast, with bulk Pd^0 almost nothing occurred. The test materials shown in Fig 4 are listed in order of decreasing lengths of their incubation periods and in order of increasing amounts of D-atoms absorbed as measured by integrated released chemical reaction energy. The sample order is:

$$Zr_3NiO (Zr^*) > ZrO_2 \cdot Pd (Pd^\circ) > Pd\text{ black} (Pd^\bullet) > bulk Pd (Pd^\circ)$$

Eq. 1

This listing order is based on the equal 3-gram weights. Here, although $Zr^* \sim Pd^\bullet = Pd^\circ = 3$ gram in weight, $ZrO_2 \sim 2$ gram, $Pd^\circ \sim 1$ gram in $ZrO_2 \cdot Pd$ which was made by oxidizing bulk amorphous alloy $Zr_{65}Pd_{35}$, and although ZrO_2 can not absorb, $Pd^\circ (= \text{nano-Pd})$ absorbs abundant D/H atoms. The Pd° contributes about one third of the weight of the $ZrO_2 \cdot Pd$, whereas the Zr^* and Pd° might be expected to contribute the majority or all of the weight in their respective powder samples.

Referenced to the active nano-metal content, the Pd⁰ might be the most absorbent powder component. However, assemblages of nano-particles cannot exist when the nano-metal components contact each other. The particles instantly change into bulk-state metal with the low absorption properties described in the introduction. This makes the nano-metal fraction uncertain. The order of Eq. 1, based on the same weight of powder sample, avoids this uncertainty. It indicates that abundant “Pycnodeuterium” is formed with both Zr* and Pd⁰.

In following section we show that solid nuclear fusion reactions occur when “Pycnodeuterium” is present in response to stimulation energy. However, in bulk Pd⁰ nothing happens. From this behavior, we understand that the great important event is formation of “Pycnodeuterium.”

Reactor Experiments

We developed the concept of a solid nuclear fusion reactor using solid Pycnodeuterium as fuel, as shown in Fig. 5. The left side illustrates the principle of the Laser Welding fusion reactor, and the right side diagram illustrates the principle of the Sono-implantation solid fusion reactor. In the Laser Welding fusion reactor, shown in the left diagram, the sample holder is an inverted triangular ditch which was machined into a solid stainless steel rod parallel to its center axis. The rod was 3 cm in diameter and 15 cm in length. A 3-gram sample of powder was dispersed along the bottom of the ditch, which extended over 10 cm. The sample holder was inserted into a quartz glass cylinder, and the inner air was evacuated so as to maintain a vacuum of 10⁻⁷ Torr extended over 2 days at 130°C. After that, D₂ gas was injected into the quartz cylinder at a constant flow rate of 20 cc/min until the inner pressure of D₂ gas built up to 10 atm. The D₂ gas inflow was absorbed as D-atoms into the

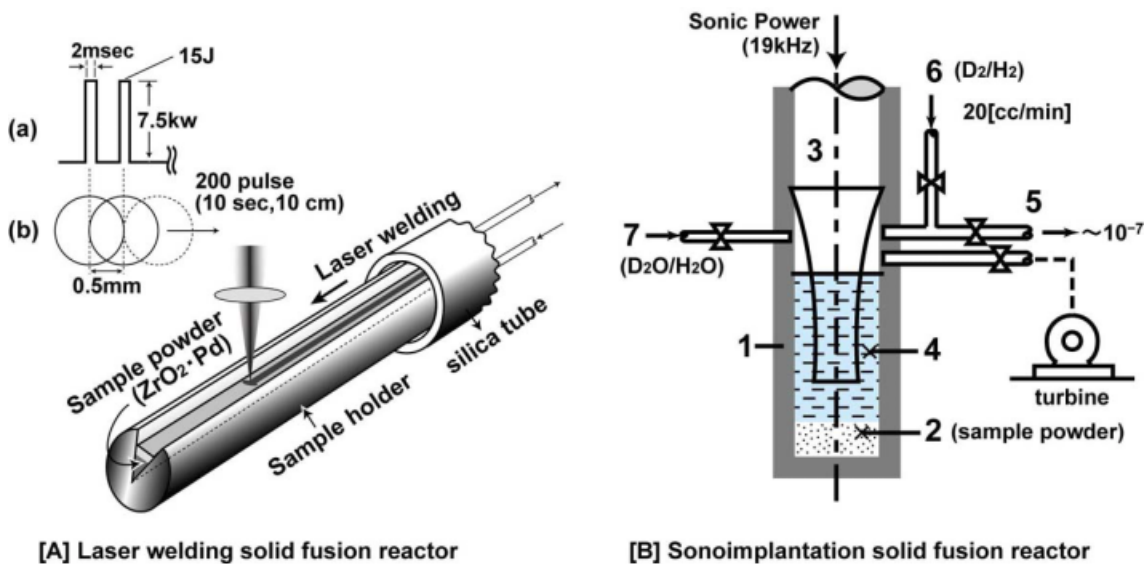


Fig. 5 Principle of solid "Pycnodeuterium" nuclear fusion reactor ("Solid fusion reactor")

sample powder and also served as a “reactor working gas.” Then, laser stimulation energy was supplied for a period of time to the solid Pycnodeuterium fuel by the usual Laser Welding process. The upper part of the diagram shows the laser wave form, which is a repeated rectangular pulse with a pulse width of 2 msec, height of 7.5 K watt, and pulse energy of 15 Joule/pulse. The pulse repetition rate was 20 pps and average power was 300 watt. The energy stimulation process lasted for 10 seconds. During this time 200 light pulses were delivered along the 10-cm ditch.

Fig. 6. shows micrographs of powder “Before” and “After” the Laser stimulation of nano Pd particles (Pd°) using D_2/H_2 gas as the reactor working gas. Left top side Photo [A] shows the “Before” sample condition, that is, it shows the original powder of $\text{ZrO}_2 \cdot \text{Pd}$ in the crushed condition of oxidized $\text{Zr}_{65}\text{Pd}_{35}$. Photo [B] is an electron micrograph of [A], which shows nano-Pd particles Pd° dispersed within a matrix of ZrO_2 for the “Before” sample. Photo [C] and Photo [D] are electron micrographs which show the “After” condition, that is, after using the Laser Welding process. Both Photo [C] and Photo [D] are to be compared with the “Before” condition of Photo [B]. Photo [C]

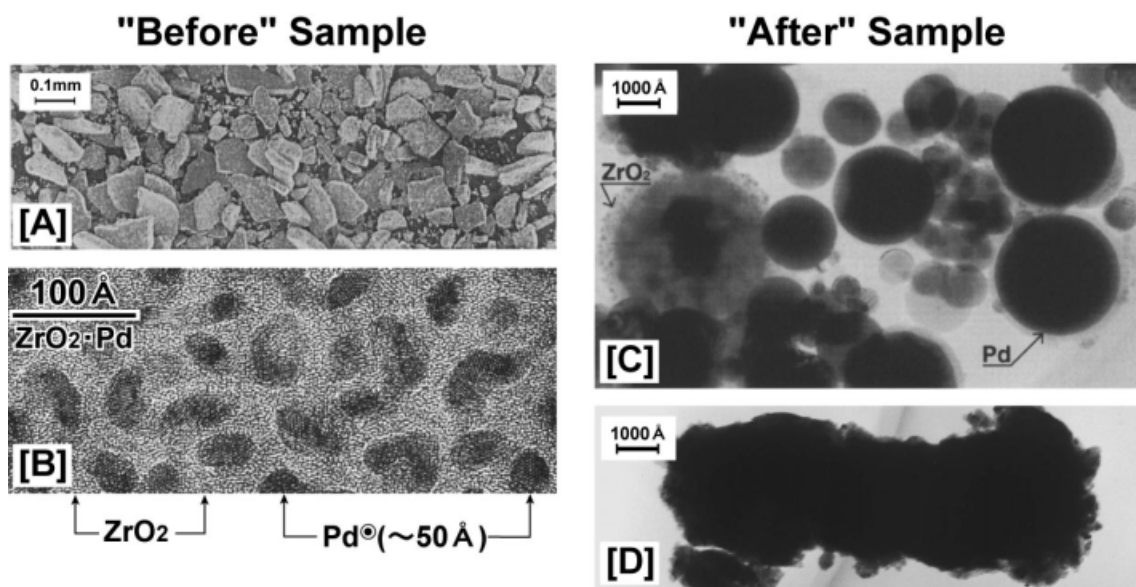


Fig. 6 Photomicrograph [A] and electron micrographs ([B], [C], [D]) of characteristics and its change of the sample powder ($\text{ZrO}_2 \cdot \text{Pd}^\circ$) using laser welding nuclear fusion system.

Note; Photo [A] : size and shape of the sample powder. Photo [B] : relation of matrix ZrO_2 and nano-Pd particles ($\sim 50 \text{ \AA}$). Photo [C] : dramatical change in size and shape after laser stimulation ("After sample") against highly deuterated sample ([A] and [B] : "Before sample"), Photo [D] shows "After" sample using H-atoms instead of D-atoms against "Before" sample. Extreme difference between [C] and [D] resulted from function of D-atoms (Pycnodeuterium) and H-atoms (Pycnohydrogen).

clearly shows that the ZrO_2 matrix and nano-Pd particles were dramatically melted, creating spherical shapes with various kinds of size, and separated from each other. In this photograph, black balls and translucent balls can be seen, with nano-Pd particles dispersed inside matrix ZrO_2 , with both instantly changed at the same time into bulk Pd and ZrO_2 , respectively. Moreover, we can see many black balls of various sizes, even inside the large translucent ZrO_2 balls.

These dramatic changes resulted from Solid Pycnodeuterium nuclear fusion. Photo [D] is substantially different from the Photo [C], even though the same process was used in both experiments. Photo [D] shows sharp edges and no balls. In Photo [D] “Pycnohydrogen” was used instead of “Pycnodeuterium.” That is to say, the working gas was H_2 instead of D_2 gas, and it never caused nuclear fusion.

Mixed Gas Studies

Based on this experiment, we have explored two important issues: 1. What kind of working gas is the best? 2. What kind of stimulation beam energy is the best to excite Pycnodeuterium? Choices include the laser, electron, plasma, neutron, and sono beam, and so on. At present we are still investigating these questions. We are testing mixed gases, not only pure D_2 , but mixtures such as $D_2 + He$ gas. As shown in Fig. 7, using pure D_2 gas and mixed $D_2 + He$ gas in conjunction with a particular composite Zr^* , evident differences appeared in D-absorption characteristics. For the same end pressure, the “constant period” was shorter with the mixed gas than with the pure D_2 gas. Another difference was a slightly lower chemical reaction rate and a slightly longer reaction period with the mixed gas. This made it necessary to raise the inner pressure in the early stages with the

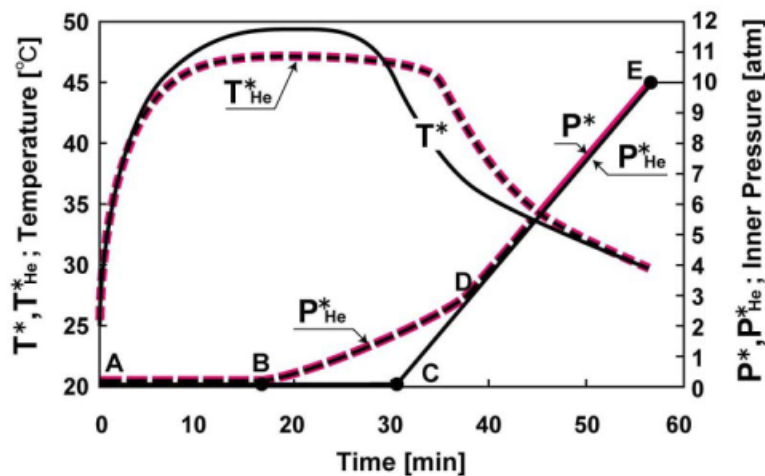


Fig. 7 Difference of Absorption characteristics of pure D_2 gas and mixed gas (pure $D_2 + 10^4$ [ppm] 4He) into Zr^* particles

Note; Pure D_2 Gas (P^* , T^*) ; Mixed Gas (P^*_{He} , T^*_{He})

mixed gas. Despite these differences, the total chemical reaction energy was the same with both working gases.

These results reveal the difficulty of D-absorption into Zr^* particles from a mixed gas as compared with pure D_2 gas. We conclude that D_2 and 4He in the mixed gas are separated at the surface of the particles. D_2 gas can easily enter into composite Zr^* as D-atoms until saturation. But He atoms can not enter, so they remain at the surface, and disturb the D_2 gas coming to contact at the surface. Until saturation of D-atoms, this event requires the use of a higher inner pressure compared with pure D_2 gas when using a mixed gas.

This conclusion was very important, and prompted a new idea, which is displayed in Fig. 8. Namely, as shown in left side diagram [A], use of pure D_2 working gas results in an ultrahigh density of D_2 molecules at the surface of the sample particles when they are saturated with D atoms. These molecules are called "boundary molecules." When using mixed $D_2 + He$ gas, as shown in the right side diagram [B], there is a corresponding ultrahigh density of He atoms concentrated at the surface of the sample particles. We called these atoms "boundary atoms." It is emphasized that the total amount of D absorbed inside each sample particle is the same for the two working gases. This is very important to understand in order to follow our thinking regarding the new experiment results. For instance, using pure D_2 working gas, the incident stimulation energy first excites "boundary molecules" and also produces excited D atoms coming from the dissociated D_2 molecules. In other words, the incident energy changes into three kinds of "boundary" energy: dissociation energy in the form of dissociated D_2 molecules, excitation energy in the form of excited D atoms, and energy delivered directly to the surface of the composite particles. In contrast, when using the mixed working gas $D_2 + He$, the incident energy changes into only two kinds of "boundary" energy: excitation energy in the form of excited He, which is excited to a relatively high excitation level, and

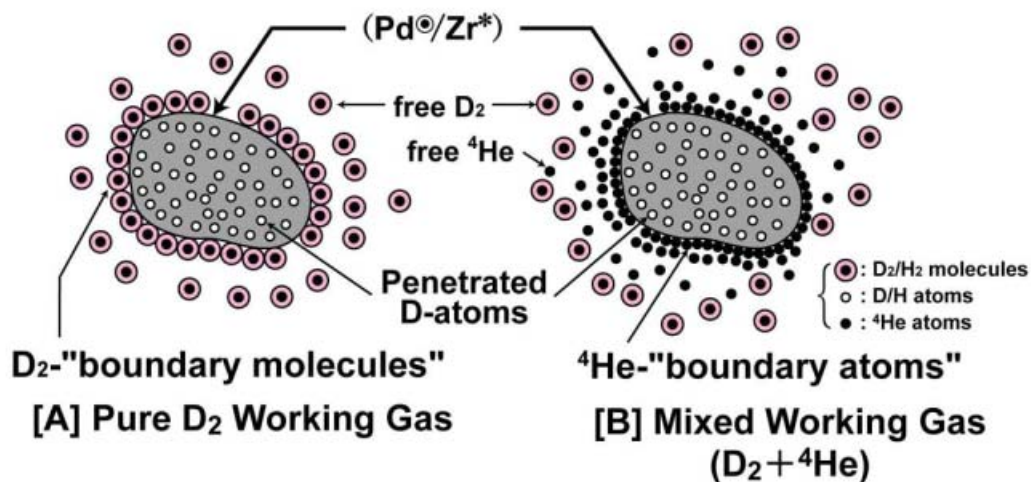


Fig. 8 Formation mechanism of "boundary molecules" and "boundary atoms".

energy delivered directly to the surface of the composite particles. As a result, the excited He compared with the excited D-atoms has a strong possibility of effectively exciting Pycnodeuterium with considerably higher energy and larger amount. Therefore, it was concluded that use of a mixed working gas compared pure D₂ gas has a greater expectation for generating strong Pycnodeuterium nuclear fusion.

Fig. 9 (next page) shows the results of the Laser Welding nuclear fusion studies. The bottom side diagrams show “absorption characteristics” of the working gases absorbed into the sample powders. The left side diagram Gas [A] shows the absorptions of pure D₂ gas and pure H₂ gas into Pd particles, respectively. The right side diagram Gas [B] shows the absorptions of two D₂ + He gas mixtures, with 10³ and 10⁴ ppm He, respectively, into 4 kinds of sample powder: Zr* from Zr₃NiO, Pd[⊙] from ZrO₂•Pd, Pd black, and bulk Pd. All powder samples were 3 grams in weight.

The upper diagrams [A₀] and [B₀] in Fig. 9 shows the amounts of ⁴He generated as a result of using the Laser Welding stimulation process, using Gas [A] and Gas [B], respectively. The vertical axis indicates “Generated He,” represented by the symbol ΔHe (“After” – “Before”), which is the difference in the amount of He “After” and “Before” Laser Welding stimulation. The calibration scale for the mass spectrometer helium data is based on a helium signal using an air sample, which contains 5.2 ppm ⁴He. In addition, when D₂ + He mixed gases are used, the “Generated He” is quantified by another symbol R_{He}, which is the “After”/ “Before” ⁴He signal ratio. The measured “Generated He ratios” are printed inside the blue circles in diagram [B₀], which is the upper-right part of Fig. 9. The horizontal axis is drawn at the “Before” condition, which corresponds to ΔHe = ~0 ppm and “Generated He-ratio” = 1.

The results of studies using pure D₂ gas in conjunction with powder samples Pd[⊙] from ZrO₂•Pd are shown in diagram [A₀], which is the upper-left part of Fig. 9. We concluded that in one test 100 ppm of ⁴He was generated by the Laser Welding stimulation. The data for a corresponding study using pure H₂ with a Pd[⊙] sample powder showed no generated ⁴He.

The results of the studies using “Mixed gas” and various powder samples are shown in diagram [B₀], which is the upper right side diagram of Fig. 9. Powder samples tested using “Mixed gas” were: Zr* from Zr₃NiO, Pd[⊙] from ZrO₂•Pd, Pd from Pd black, and bulk Pd. Zr* and Pd[⊙] caused abundant ⁴He, such as around 105 ppm. But in spite of using the same conditions, much less ⁴He was generated in Pd black and no ⁴He was generated in bulk Pd.

The Laser Welding process was developed by us in 1966, and was the first such process in the world.

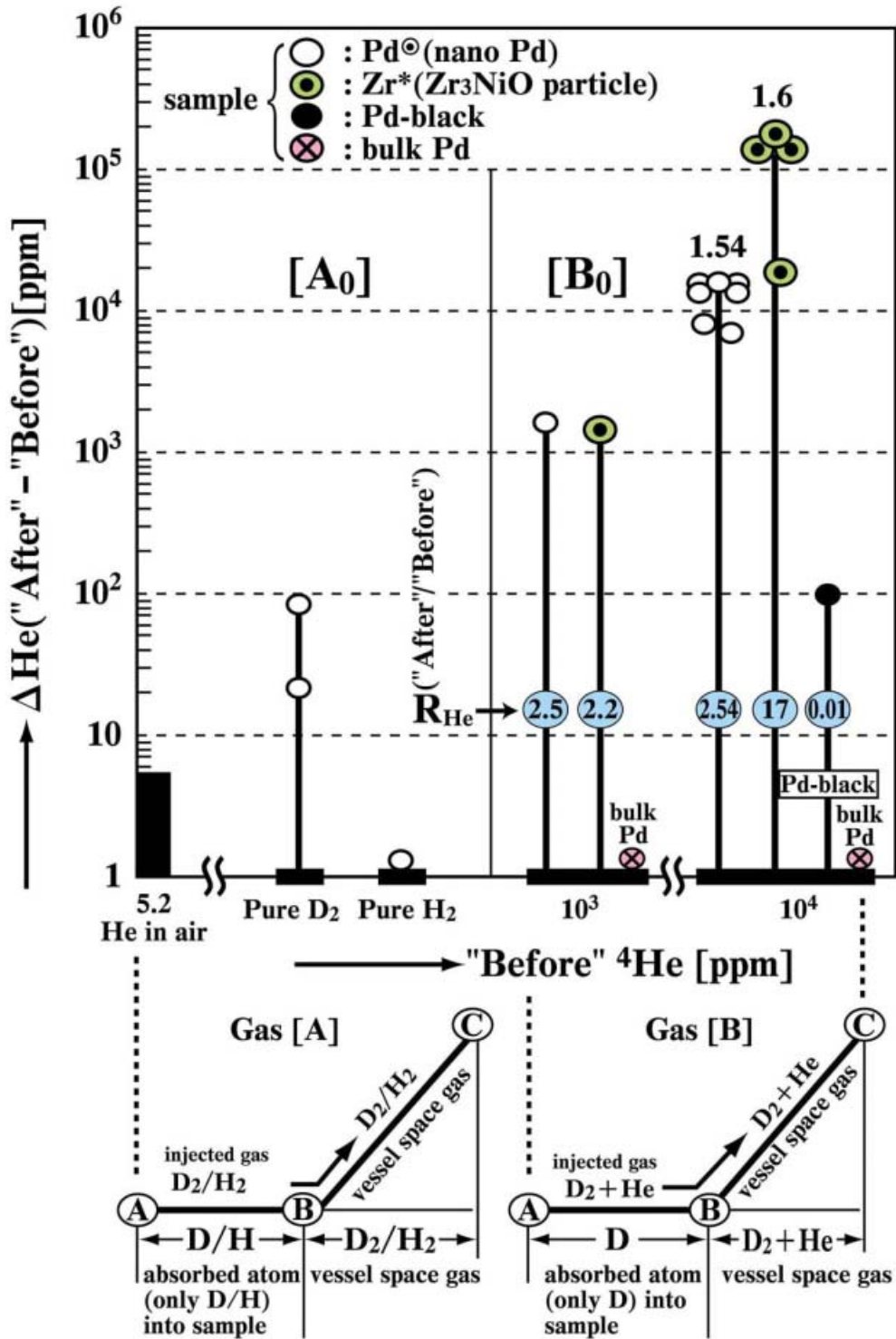


Fig. 9 Experimental conditions and results in Laser Welding Nuclear Fusion using reactant sample (○Pd[⊙], ●Zr*, ●Pd black, ⊗ bulk Pd).

Note: $\begin{cases} \text{Generated He} : \Delta\text{He} \equiv \text{"After"} - \text{"Before"} \\ \text{Generated He-ratio} : R_{\text{He}} \equiv \text{"After"} / \text{"Before"} \end{cases}$

Sono-implantation nuclear fusion

The following results of Sono-implantation nuclear fusion are presented. We introduced the term of “sono-implantation,” and published in *Proc. Japan Acad.* 4 times beginning in 1998, and 2 times in *Appl. Phys. Lett.* (USA) and in *Proc. ICCF9* last year. The key point in sono-implantation is that all kinds of gaseous atoms can be easily implanted into all kinds of metal particles using the sono-implantation effect. Fig. 5 [B] illustrates the principle of the Sono-implantation solid fusion reactor. Marks 1-4 identify a closed vessel, reactant sample, ultrasonic vibrator, and sonic transfer medium D₂O or H₂O for the ultrasonic beam. Marks 5-7 identify pipes for evacuation, reactor working gas injection, and liquid injection of D₂O and H₂O. To begin a test, a reactant sample is placed on the bottom of the closed vessel. Then the inner air is evacuated so as to keep the pressure below 10⁻⁷ Torr for a period of 2 ~ 3 days at 150°C. After that, pure D₂ gas is injected into the closed vessel through pipe 6 with a fixed flow rate V_G (=20 cc/min) until the inner pressure P_{in} reaches 10 atm. Then, D₂O/H₂O liquid is injected by pipe 7 into the closed vessel. In the tests providing the data shown in Fig. 10 (next page), sono-power of 300 watt at 19 kHz was used for about one hour and directed against samples of Pd powder and Pd black, respectively. Mixed gases, D₂ + 400, 10³, or 10⁴ ppm He, were used with Pd and Pd black for bottom-left chart labeled “Gas [C].” Mixed gases, H₂ + 400 ppm He and H₂ + 10⁴ ppm He, were used for bottom-right chart labeled “Gas [D].” These gases were injected into the reactor vessel in the same way as employed in the Laser Welding process.

Again referring to Fig. 10, the data displayed in the upper-left side chart [C₀] tested Gas [C] in conjunction with Pd-black, and also in conjunction with several powder samples Pd[®] from ZrO₂•Pd. Tests with the D₂ + He mixed gases showed “Generated He ratios” as high as almost 30, relative to the initially present He. Tests with the H₂ + He mixed gases were also carried out, and also a test with D₂ gas mixed with 7% H₂. When the mixtures containing H₂ were used, no “Generated He” was detected, as shown in upper right side [D₀].

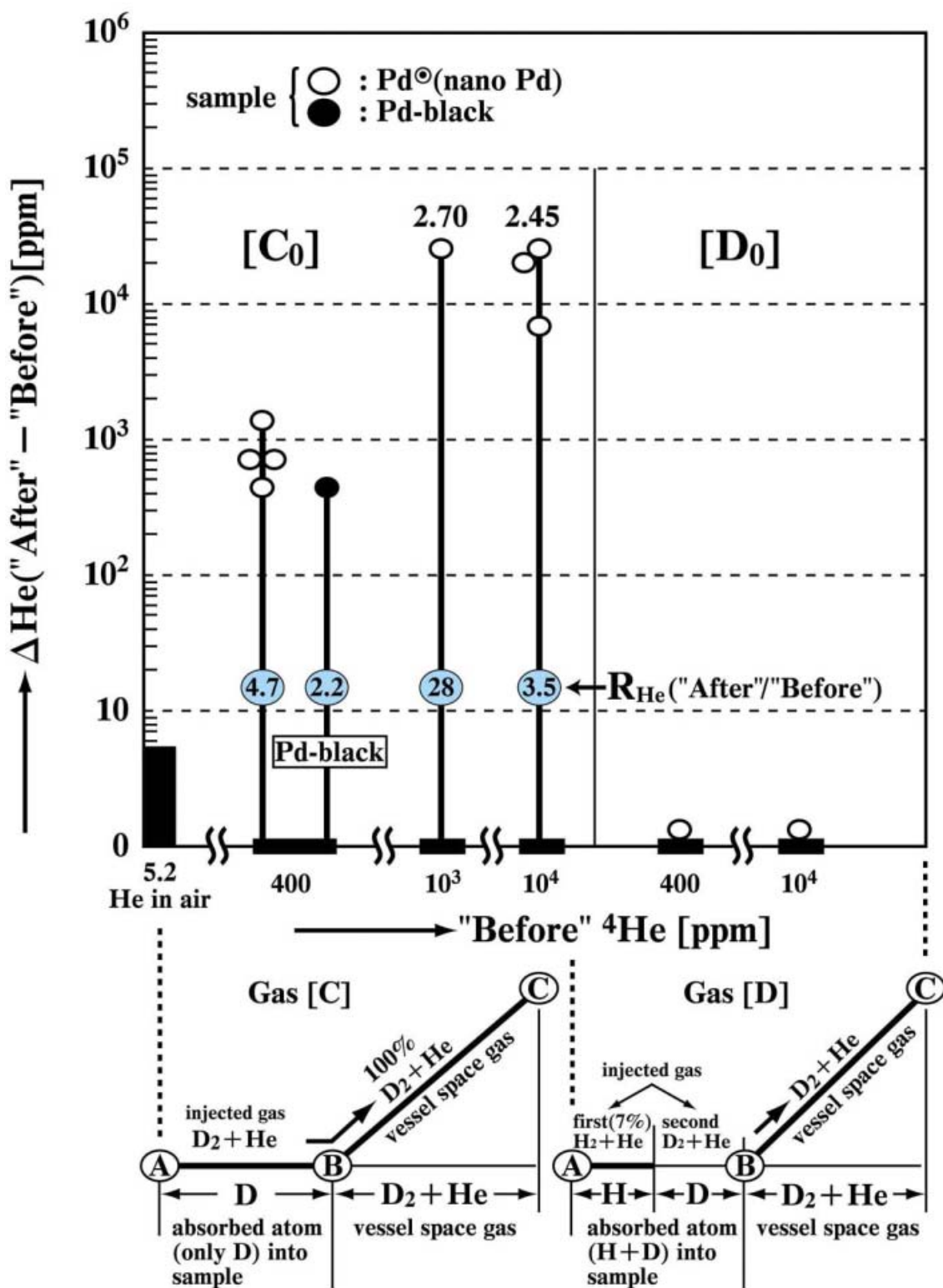


Fig. 10 Experimental conditions and results in Sonoimplantation Nuclear Fusion using reactant sample (○Pd[⊙], ● Pd black) and mixed gas (D₂+x[ppm]⁴He, here, x=400 ; 10³ ; 10⁴)

Conclusions

- 1) Pycnohydrogen (ultrahigh density of hydrogen-lumps) never causes the nuclear fusion reaction.
- 2) Bulk metal never causes Pycnodeuterium, hence never causes the fusion reaction.
- 3) If materials easily form solid Pycnodeuterium, then they can cause strong solid nuclear fusion.
- 4) Solid Pycnodeuterium is by far the most excellent fuel for nuclear fusion, as compared with gaseous deuterium as used in thermonuclear fusion. Thermonuclear fusion requires an ultra high temperature plasma. Because a high temperature plasma requires high temperature, low density electrons, there is an excessively large “Debye-shielding length” and no neutralizing zone. The D-ion space charge becomes too large, just as in the vacuum state.

At the present, two methods using laser stimulation energy are used to cause thermonuclear reaction, as shown in Fig. 11 (next page). One is to use an extremely high power pulsed laser “implosion” system, which is well known in general and which was illustrated in a *Nature* cover in 1986. Results obtained by the newest system were described in *Nature* last year. Results corresponding to the highest reported input power are shown in “blue color” in the [notice] portion of upper table of Fig. 11. These data were obtained using an input pulse with a pulse power of 10^{19} watt/50-ps. The plasma temperature was 10^4 ev and the number of generated particles was 10^{13} per pulse. As shown in red color, using an input pulse with pulse power of 10^{15} watt over a 1-ps period, the plasma temperature was 10^3 ev and the number of generated particles was 10^5 /pulse. This is the latest report for thermonuclear fusion using “gaseous deuterium” as fuel. In contrast, there is the Laser Welding nuclear fusion system using “solid Pycnodeuterium” as fuel. Our Laser implosion system used only 300 watt and generated about 10^{19} to 10^{20} particles per 10 seconds. It is concluded that “solid Pycnodeuterium” with stimulation energy is by far the more excellent fusion fuel as compared with “gaseous deuterium as used in thermonuclear fusion.” It is, therefore considered worth while to test the “solid fuel” against the “gaseous fuel” using various stimulation energy systems, including the laser system. We think such testing is very important.

Newest Type Laser Implosion System Thermonuclear Fusion

| Target | Ei, no. of beams | Es | Yield neutron number ↓ Ny |
|----------------------|------------------|-----|---------------------------------|
| Cone+shell | 1.2 kJ, 9 beams | 60J | $(1-3) \times 10^5$ |
| Cone+shell | 1.2 kJ, 9 beams | 0 | $(0.8-1) \times 10^4$ |
| Spherical shell only | 2.6 kJ, 12 beams | 0 | $(2-3) \times 10^5$ |

[Notice] Input ; $10^{15} \sim (10^{19})$ [watt], Temp ; $10^3 \sim (10^4)$ [eV]
 Effective period ; $1 \sim (50)$ [p.s], Pressure ; $60 \sim (600) \times$ (metal density)
 Generated particles ; $10^5 \sim (10^{13})$ / Pulse
 () : Max. value (blue color) ; **Newest system (red color)**

Note 1) "Nature" ; Vol.412, No.6849, pp.798-802 (2001)
 Vol.418, No.6901, pp.933-934 (2002)

Note 2) "Research" ; Institute of Laser Engineering, Osaka Univ.

Laser Welding System Solid Fusion

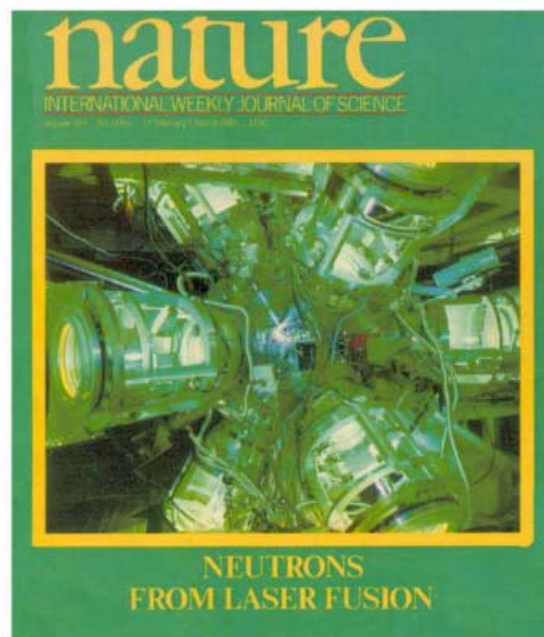
[Notice]

Input ; **300 [watt]**

Effective period ; **10 [sec]**

Pressure ; D_2/H_2 gas 10[atm]

Generated particles ;
 $10^{19} \sim 10^{20}$



"Nature Cover"
 (Laser Implosion System
 developed in OSAKA UNIV.)

Fig 11. Comparison of Laser implosion nuclear fusion using gaseous deuterium and Laser welding nuclear fusion using solid Pycnodeuterium as nuclear fuel.

Acknowledgments

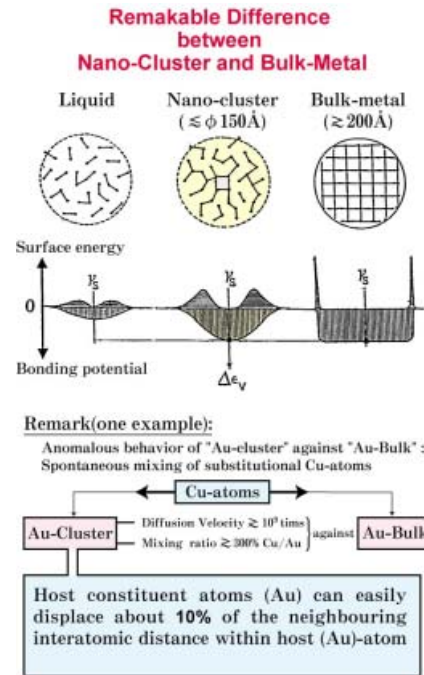
The authors would like to thank Dr. T. Yamazaki, Professors Emeritus at the University of Tokyo, Dr. H. Fujita, Professor Emeritus at Osaka University, Dr. A. Inoue, Professor of Tohoku University, Dr. M. Futamata, Professor of Kitami Institute of Technology, Dr. J. Morimoto, Professor of Kinki University, and electron microscopy specialist E. Taguchi, Osaka University, for their kind cooperation.

References

- 1) Arata, Y., and Zhang, Y.-C.: Kakuyugo Kenkyu (J. Japan Soc. Plasma Sci. and Nucl. Fusion Research) **62**, 398 (1989); **67**, 432 (1992); **69**, 963 (1993). Proc. ICCF4 (1993), Fusion Technology, **18**, 95 (1990); **22**, 287 (1992); Proc. Japan Acad. **66B**, 1-6 (1990); **70B**, 106, (1994); **71B**, 98, (1995); **71B**, 304, (1995); **78B**, 57, (2002). **78B**, 63, (2002); Jpn. J. Appl. Phys., **37** (1998) L1274; **38** (1999) L774. High Temp. Soc. Jpn., **Vol. 23** (Special Vol.), 1-56.
- 2) Arata, Y., and Zhang, Y.-C. (1998) Proc. Japan Acad. **70B**, 106, (1994); **71B**, 98, (1995); High Temp. Soc. Jpn, (Special Vol.) 1-56 (1997).
- 3) Arata, Y., and Zhang, Y.-C. Proc. Japan Acad., **78B**, (2002); Proc. ICCF9 (2002); Yamamura, S., Sasamori, K., Kimura, H., Inoue, A., Zhang, Y. C., and Arata. Y.; J. Mater. Res., **Vol. 17** No.6 (2002); Arata, Y., Zhang, Y. C., Fujita, H., Inoue, A., High Temp. Soc. Jpn, **Vol. 29**, No.2 (2003).

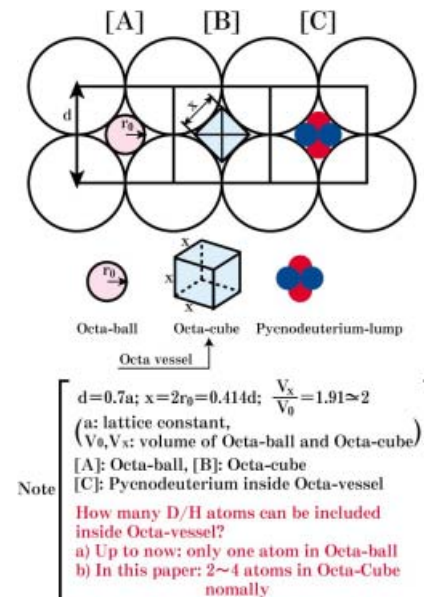
Appendix I: The whys and wherefores of the distinguished difference between nano-state and bulk-state in metals against movability and absorbent of D / H atoms within their metal-states.

Characteristics of each state (Liquid, nano-cluster, and bulk-material) were illustrated with allowable range in size originated from both of their surface energy and bonding potential in the upper side diagram of right side figure. As a result, nano-cluster display a structure similar to that of liquid, and the most important point is that nano particles can absorb instantly other atoms. That is to say, nano particle display “spontaneous mixing action”, but in the bulk metal, practically no mixing action. Neighboring atoms are joined just as with a spring connecting them, with easily mobility at 10%, as shown in lower side diagram of right side figure. These nano and bulk states are formed with the same atoms, but material in the states acts as if it was completely different material.



Appendix II: The whys and wherefores of closely connected relation between the construction of octahedral inner space within phase centered cubic Pd lattice and ultrahigh density of D/H atoms solidified as “Pycnodeuterium/Pycnohydrogen” inside their inner space.

Up to now, it has been thought in general that only one D/H atom enter into inner contacted ball (shortly “Octa-ball”) against Octahedral inner space as shown in left side [A]-diagram in the right side figure. But we thought “Octa-cube” as shown in [B]-diagram in stead of Octa-ball in [A]. As a result, 4 D/H atoms enter into Octa-cube, and then Octa-cube is called “Octa-vessel”.



Namely, assemblage of 4 D/H-atoms are solidified with ultrahigh density as “Pycnodeuterium/Pycnohydrogen” inside Octa-vessel as shown in right side [C]-diagram.

Appendix III: Indication of absorption amount of D/H atoms and their location inside nano and bulk Pd lattice using Octa-vessel.

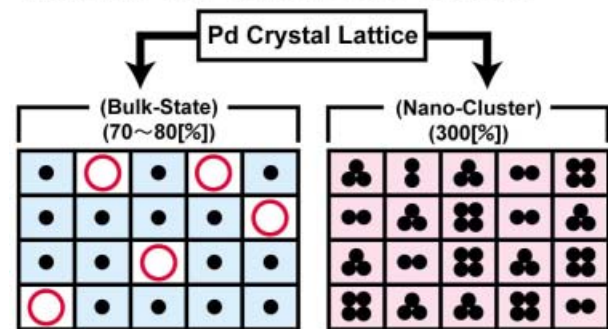
Using concept of Octa-vessel, crystal lattice can be expressed by assemblage of connected Octa-vessel (the “Octa -lattice”) as shown in right side figure. The left side in this figure shows bulk-state saturated with 80% D/H atoms and right side shows nano-state with “Pycnodeuterium/Pycnohydrogen”.

Under both of these saturated situations, D/H atoms cannot move to get over from Octa-vessel to other one. This means that D/H atoms in nano-state can be easily solidified to form

“Pycnodeuterium/Pycnohidrogen”

inside Octa-vessel, and “Pycnodeuterium” cause easily cause solid state nuclear fusion, but “Pycnohydrogen” cannot. On the contrary, in the bulk-state deuterium can never cause any of these events. The most important point basically is that new material to induce nuclear fusion should have the largest quantity of D-atoms possible, and such materials at below 100% concentration D-atoms are essentially useless, just as bulk metals are.

Relation of distributed solid deuterium between "bulk-state" and "nano-clusters" in metal



Model diagram of deuterated Pd crystal lattice using Octa-vessel included solidified "Pycnodeuterium"

Note

- • • • : Each mark show the number of solidified D/H atoms (1~4 atoms) inside Oct-vessel
- Mark, ○ : nothing any atom inside Octa-vessel
- a) Nano-cluster : Constructed with Octa-vessel included solidified Pycnodeuterium/Pycnohydrogen (2~4 atoms)
- b) Bulk-state : constructed with Octa-vessel included both of only one atom and nothing any atom, and each atom can not move from Octa-vessel to other one.
- c) When solid nuclear fusion will be induced inside Octa-vessel, it can be easily understanding that nuclear reaction generate at the Pycnodeuterium in nano-cluster, but nothing at the Pycnohydrogen and also in the bulk-state